Asymmetric nuclear matter in a parity doublet model with hidden local symmetry

Yuichi Motohiro,[1] Youngman Kim,[2] and Masayasu Harada[1]
[1]*Department of Physics, Nagoya University, Nagoya 464-8602, Japan*
[2]*Rare Isotope Science Project, Institute for Basic Science, Daejeon 305-811, Korea*
(Received 11 May 2015; published 3 August 2015)

We construct a model to describe dense hadronic matter at zero and finite temperatures, based on the parity doublet model of DeTar and Kunihiro [C. E. DeTar and T. Kunihiro, Phys. Rev. D **39**, 2805 (1989)], including the isosinglet scalar meson σ as well as ρ and ω mesons. We show that, by including a six-point interaction of the σ meson, the model reasonably reproduces the properties of normal nuclear matter with the chiral invariant nucleon mass m_0 in the range from 500 to 900 MeV. Furthermore, we study the phase diagram based on the model, which shows that the value of the chiral condensate drops at the liquid-gas phase transition point and at the chiral phase transition point. We also study asymmetric nuclear matter and find that the first-order phase transition for the liquid-gas phase transition disappears in asymmetric matter and that the critical density for the chiral phase transition at nonzero density becomes smaller for larger asymmetry.

DOI: 10.1103/PhysRevC.92.025201 PACS number(s): 21.65.Cd, 21.65.Mn, 12.39.Fe

I. INTRODUCTION

With the advent of the next generation radioactive beam facilities, isospin asymmetric nuclear matter claims much attention in contemporary nuclear physics. At those facilities we could create terrestrial environments to study dense matter with a large neutron or proton excess through nuclear reactions with radioactive nuclei.

Studying nuclear matter is also important to understand the structure of neutron stars [1]. In 2010 and 2013, two neutron stars with twice solar mass were found [2,3] and many models yielding the soft equation of states (EOS) were excluded. Neutron stars offer very cold and asymmetric dense environments and may have hyperons in the core of the stars. If there are hyperonic degrees of freedom, it is expected that the EOS becomes softer and the neutron star mass becomes lighter. Another important astrophysical site for nuclear matter is a hybrid star whose center has quark matter [4].

The properties of asymmetric matter have been investigated in various approaches [5–14]. Very recently the liquid-gas and chiral phase transition have been studied in a parity doublet model with a six-point scalar interaction in which mesonic fluctuations are included by means of the functional renormalization group [15]. Several studies on the isospin asymmetric dense matter have been done in the framework of the parity doublet model (mirror assignment) [16,17]: The properties of symmetric dense matter such as chiral phase transition have been extensively studied in the parity doublet models at zero or finite temperatures [18–27]. In Refs. [18–27], the authors discussed the chiral invariant mass and the incompressibility K of nuclear matter and they reproduce the empirical value $K = 240 \pm 20$ MeV (taken from, for example, Refs. [28,29]) only when the chiral invariant mass is close to the nucleon's mass, $m_0 \sim 900$ MeV. On the other hand, in Ref. [17] the authors determined m_0 from the decay width of $N^* \to N\pi$ to be $m_0 = 270$ MeV, while in Ref. [22] they used the decay modes of $N^* \to N\pi$ and $a_1 \to \pi\gamma$ to obtain $m_0 \sim 500$ MeV. Though m_0 may change in dense matter, it is hard to understand why the value of m_0 is in such variety, which motivates us to seek how to reproduce the normal nuclear matter properties with a medium chiral invariant mass.

In this paper, we extend the parity doublet model by including ρ and ω mesons through the hidden local symmetry. For earlier works on this extension, we refer the reader to Refs. [30–32]. We extend this model further by adding a six-point interaction of a scalar meson, which allows us to vary the value of the chiral invariant mass in the range of $m_0 \geqslant 500$ MeV. Here, as a first step, we do not consider hyperonic matter and work within the mean-field approximation. Then, we determine our model parameters, except the chiral invariant mass (m_0), by performing global fitting to physical inputs (masses and pion decay constants in free space and nuclear matter properties). We then study the EOS and the phase diagram of dense matter at finite temperature. We find that the predicted slope parameter at the saturation density meets the constraint from heavy ion experiments and neutron star observations (see, e.g., Refs. [33,34]) and observe that the chiral condensate drops at the chiral and liquid-gas transition points. It is also seen that smaller m_0 values prefer smaller critical densities for the chiral phase transition. The study of asymmetric matter reveals that the first-order nature of the liquid-gas transition disappears in asymmetric matter and the critical densities for the chiral transition become smaller with increasing asymmetries, which is consistent with previous studies.

In Sec. II we extend the parity doublet model, and in Sec. III we fix the model parameters. Our results on the bulk properties of nuclear matter and density dependence of chiral condensate and nucleon mass are given in Sec. IV. We present the phase diagram of dense (asymmetric) matter in Sec. V. Finally, the conclusion and discussion follow in Sec. VI.

II. EXTENDED PARITY DOUBLET MODEL

We construct a chiral effective model based on the parity doublet model [16,17], in which a nucleon with positive parity is regarded as a chiral partner to the one with negative parity and they belong to the same multiplet. The transformation

properties of the positive- and negative-parity nucleon fields are given by

$$\psi_{1r} \to g_R \psi_{1r}, \quad \psi_{1l} \to g_L \psi_{1l}, \tag{2.1}$$

$$\psi_{2r} \to g_L \psi_{2r}, \quad \psi_{2l} \to g_R \psi_{2l}, \tag{2.2}$$

where g_R (g_L) is an element of the $\mathrm{SU}(2)_R$ [$\mathrm{SU}(2)_L$] chiral symmetry group, and ψ_{1r} and ψ_{2r} (ψ_{1l} and ψ_{2l}) are the right-handed (left-handed) fields projected as

$$\psi_{1r,2r} = P_R\, \psi_{1,2}, \quad \psi_{1l,2l} = P_L\, \psi_{1,2},$$
$$P_{R,L} = \frac{1 \pm \gamma_5}{2}. \tag{2.3}$$

To construct a linear σ model including these nucleon fields, we introduce the following field:

$$M = \sigma + i\vec{\pi} \cdot \vec{\tau}, \tag{2.4}$$

where σ denotes an isosinglet scalar field, $\vec{\pi}$ the pion field, and $\vec{\tau}$ the Pauli matrices. The chiral transformation property of M is given by

$$M \to g_L M g_R^\dagger. \tag{2.5}$$

By using these fields, the Lagrangian of a linear σ model type is expressed as[1]

$$\begin{aligned}\mathcal{L}_N =\ & \bar{\psi}_{1r} i\gamma^\mu D_\mu \psi_{1r} + \bar{\psi}_{1l} i\gamma^\mu D_\mu \psi_{1l} \\ & + \bar{\psi}_{2r} i\gamma^\mu D_\mu \psi_{2r} + \bar{\psi}_{2l} i\gamma^\mu D_\mu \psi_{2l} \\ & - m_0[\bar{\psi}_{1l}\psi_{2r} - \bar{\psi}_{1r}\psi_{2l} - \bar{\psi}_{2l}\psi_{1r} + \bar{\psi}_{2r}\psi_{1l}] \\ & - g_1[\bar{\psi}_{1r} M^\dagger \psi_{1l} + \bar{\psi}_{1l} M \psi_{1r}] \\ & - g_2[\bar{\psi}_{2r} M \psi_{2l} + \bar{\psi}_{2l} M^\dagger \psi_{2r}],\end{aligned} \tag{2.6}$$

where m_0 is the chiral invariant mass, g_1 and g_2 are the coupling constants, and the covariant derivatives include the external gauge fields $\mathcal{R}_\mu$ and $\mathcal{L}_\mu$ as

$$D_\mu \psi_{1r,2l} = (\partial_\mu - i\mathcal{R}_\mu)\psi_{1r,2l},$$
$$D_\mu \psi_{1l,2r} = (\partial_\mu - i\mathcal{L}_\mu)\psi_{1l,2r}. \tag{2.7}$$

The meson part of the Lagrangian is given by

$$\mathcal{L}_M = \tfrac{1}{4}\mathrm{tr}[\partial_\mu M \partial^\mu M^\dagger] - V_M - V_{\mathrm{SB}}, \tag{2.8}$$

where the meson potential V_M and the explicit chiral symmetry breaking potential V_{SB} are

$$V_M = -\tfrac{1}{4}\bar{\mu}^2 \mathrm{tr}[MM^\dagger] + \tfrac{1}{16}\lambda\{\mathrm{tr}[MM^\dagger]\}^2 - \tfrac{1}{48}\lambda_6\{\mathrm{tr}[MM^\dagger]\}^3, \tag{2.9}$$

$$V_{\mathrm{SB}} = -\tfrac{1}{4}\varepsilon(\mathrm{tr}[\mathcal{M}^\dagger M] + \mathrm{tr}[\mathcal{M}M^\dagger]). \tag{2.10}$$

[1]This Lagrangian is rewritten into a more familiar form in the literatures as

$$\begin{aligned}\mathcal{L}_N =\ & \psi_1 i\gamma^\mu \partial_\mu \psi_1 + \bar{\psi}_2 i\gamma^\mu \partial_\mu \psi_2 - m_0(\bar{\psi}_1\gamma_5\psi_2 - \bar{\psi}_2\gamma_5\psi_1) \\ & - g_1\bar{\psi}_1(\sigma + i\gamma_5\vec{\pi}\cdot\vec{\tau})\psi_1 - g_2\bar{\psi}_2(\sigma - i\gamma_5\vec{\pi}\cdot\vec{\tau})\psi_2.\end{aligned}$$

Here $\mathcal{M}$ is the quark mass matrix given as

$$\mathcal{M} = \begin{pmatrix} m_u & 0 \\ 0 & m_d \end{pmatrix} \tag{2.11}$$

and ε is a constant of mass dimension two. In the present analysis, we neglect the isospin breaking effect due to the mass difference of up and down quarks and take $m_u = m_d = \bar{m}$. It should be noticed that the potential V_M includes the dimension-six term, which will play a very important role in reproducing the properties of the normal nuclear matter with a rather wide range of the chiral invariant nucleon masses. (See next section.) When $\lambda_6 > 0$, the potential $V_M + V_{\mathrm{SB}}$ is not bounded from below. In the present analysis, we determine the vacuum in the following way: We first solve the stationary condition of the potential. When there is more than one solution, we choose the one with the lowest energy at the stationary point.

We next include ρ and ω mesons into the model based on the hidden local symmetry (HLS) theory [35–37]. The HLS is introduced by performing the polar decomposition of the field M as

$$M = \xi_L \sigma \xi_R = \sigma \xi_L^\dagger \xi_R = \sigma U, \tag{2.12}$$

where σ is a scalar meson field and ξ_L and ξ_R transform as

$$\xi_{L,R} \to h_\omega h_\rho \xi_{L,R} g_{L,R}^\dagger, \tag{2.13}$$

with $h_\omega \in \mathrm{U}(1)_{\mathrm{HLS}}$ and $h_\rho \in \mathrm{SU}(2)_{\mathrm{HLS}}$. In the unitary gauge, ξ_R and ξ_L are parametrized as

$$\xi_R = \xi_L^\dagger = \exp(i\pi^a T^a / f_\pi), \tag{2.14}$$

where $T^a = \tau_a/2$ ($a = 1,2,3$), with τ_a being the Pauli matrix. In the HLS, the vector mesons are introduced as the gauge bosons of the HLS which transform as

$$\omega_\mu \to h_\omega \omega_\mu h_\omega^\dagger + \frac{i}{g_\omega}\partial_\mu h_\omega h_\omega^\dagger, \tag{2.15}$$

$$\rho_\mu \to h_\rho \rho_\mu h_\rho^\dagger + \frac{i}{g_\rho}\partial_\mu h_\rho h_\rho^\dagger, \tag{2.16}$$

where g_ω and g_ρ are the corresponding gauge coupling constants.

To construct a model Lagrangian with the HLS, it is convenient to introduce the following one-forms:

$$\hat{\alpha}_\perp^\mu \equiv \frac{1}{2i}[D^\mu \xi_R \xi_R^\dagger - D^\mu \xi_L \xi_L^\dagger],$$
$$\hat{\alpha}_\parallel^\mu \equiv \frac{1}{2i}[D^\mu \xi_R \xi_R^\dagger + D^\mu \xi_L \xi_L^\dagger], \tag{2.17}$$

where the covariant derivatives are given as

$$D^\mu \xi_L = \partial^\mu \xi_L + i g_\rho \rho^\mu \xi_L + i g_\omega \omega^\mu \xi_L + i \xi_L \mathcal{L}^\mu,$$
$$D^\mu \xi_R = \partial^\mu \xi_R + i g_\rho \rho^\mu \xi_R + i g_\omega \omega^\mu \xi_R + i \xi_R \mathcal{R}^\mu. \tag{2.18}$$

Now, the mesonic part of the Lagrangian extended by the HLS is expressed as

$$\begin{aligned}\mathcal{L}_M = &\frac{1}{2}\partial_\mu\sigma\partial^\mu\sigma + \sigma^2\mathrm{tr}[\hat{\alpha}_{\perp\mu}\hat{\alpha}_\perp^\mu] - V_\sigma - V_{\rm SB}\\ &+ \frac{m_\rho^2}{g_\rho^2}\mathrm{tr}[\hat{\alpha}_{\parallel\mu}\hat{\alpha}_\parallel^\mu] + \left(\frac{m_\omega^2}{2g_\omega^2} - \frac{m_\rho^2}{2g_\rho^2}\right)\mathrm{tr}[\hat{\alpha}_{\parallel\mu}]\mathrm{tr}[\hat{\alpha}_\parallel^\mu]\\ &- \frac{1}{2g_\rho^2}\mathrm{tr}[\rho_{\mu\nu}\rho^{\mu\nu}] - \left(\frac{1}{4g_\omega^2} - \frac{1}{4g_\rho^2}\right)\mathrm{tr}[\omega_{\mu\nu}]\mathrm{tr}[\omega^{\mu\nu}],\end{aligned} \tag{2.19}$$

where the first line is from Eq. (2.8) with the following form of the potential:

$$V_\sigma = -\tfrac{1}{2}\bar{\mu}^2\sigma^2 + \tfrac{1}{4}\lambda\sigma^4 - \tfrac{1}{6}\lambda_6\sigma^6, \tag{2.20}$$

$$V_{\rm SB} = -\tfrac{1}{4}\bar{m}\epsilon\sigma\,\mathrm{tr}[U + U^\dagger]. \tag{2.21}$$

The second and third lines contain the mass and kinetic terms of vector mesons, respectively.

We also rewrite the nucleon part of the Lagrangian as

$$\begin{aligned}\mathcal{L}_N = &\bar{\psi}_{1r}i\gamma^\mu D_\mu\psi_{1r} + \bar{\psi}_{1l}i\gamma^\mu D_\mu\psi_{1l}\\ &+ \bar{\psi}_{2r}i\gamma^\mu D_\mu\psi_{2r} + \bar{\psi}_{2l}i\gamma^\mu D_\mu\psi_{2l}\\ &- m_0[\bar{\psi}_{1l}\psi_{2r} - \bar{\psi}_{1r}\psi_{2l} - \bar{\psi}_{2l}\psi_{1r} + \bar{\psi}_{2r}\psi_{1l}]\\ &- g_1\sigma[\bar{\psi}_{1r}U^\dagger\psi_{1l} + \bar{\psi}_{1l}U\psi_{1r}]\\ &- g_2\sigma[\bar{\psi}_{2r}U\psi_{2l} + \bar{\psi}_{2l}U^\dagger\psi_{2r}]\\ &- a_{\rho NN}[\bar{\psi}_{1l}\gamma^\mu(\xi_L^\dagger\hat{\alpha}_{\parallel\mu}\xi_L)\psi_{1l} + \bar{\psi}_{1r}\gamma^\mu(\xi_R^\dagger\hat{\alpha}_{\parallel\mu}\xi_R)\psi_{1r}]\\ &- a_{\rho NN}[\bar{\psi}_{2l}\gamma^\mu(\xi_R^\dagger\hat{\alpha}_{\parallel\mu}\xi_R)\psi_{2l} + \bar{\psi}_{2r}\gamma^\mu(\xi_L^\dagger\hat{\alpha}_{\parallel\mu}\xi_L)\psi_{2r}]\\ &- a_{0NN}\,\mathrm{tr}[\hat{\alpha}_{\parallel\mu}]\,(\bar{\psi}_{1l}\gamma^\mu\psi_{1l} + \bar{\psi}_{1r}\gamma^\mu\psi_{1r}\\ &+ \bar{\psi}_{2l}\gamma^\mu\psi_{2l} + \bar{\psi}_{2r}\gamma^\mu\psi_{2r}).\end{aligned} \tag{2.22}$$

The vacuum expectation value (VEV) of the σ field, denoted by σ_0, is determined by the stationary condition for the potential, as we explained above. The nonzero σ_0 breaks the chiral symmetry spontaneously and generates the masses of nucleons as

$$\mathcal{L}_{\rm mass} = -(\bar{\psi}_1 \quad \bar{\psi}_2)\begin{pmatrix} g_1\sigma_0 & m_0\gamma_5 \\ -m_0\gamma_5 & g_2\sigma_0\end{pmatrix}\begin{pmatrix}\psi_1\\ \psi_2\end{pmatrix}. \tag{2.23}$$

We obtain the masses of the positive-parity and negative-parity nucleons by diagonalizing the mass matrix. Here, we write the mass eigenstates as N_+ and N_-, which are related to ψ_1 and ψ_2 as

$$\begin{pmatrix}N_+\\ N_-\end{pmatrix} = \begin{pmatrix}\cos\theta & \gamma_5\sin\theta\\ -\gamma_5\sin\theta & \cos\theta\end{pmatrix}\begin{pmatrix}\psi_1\\ \psi_2\end{pmatrix}, \tag{2.24}$$

where θ is the mixing angle given by

$$\tan 2\theta = \frac{2m_0}{(g_1+g_2)\sigma_0}. \tag{2.25}$$

The mass eigenvalues are determined as

$$m_\pm = \tfrac{1}{2}\left(\sqrt{(g_1+g_2)^2\sigma_0^2 + 4m_0^2} \mp (g_1-g_2)\sigma_0\right), \tag{2.26}$$

where m_+ and m_- are the masses of positive- and negative-parity baryons, respectively.[2] From this expression, one can easily see that the spontaneous chiral symmetry breaking is responsible for the mass differences of the parity partners.

TABLE I. Determined model parameters for given m_0. Here $m_\omega = 783$ MeV, $m_\rho = 776$ MeV, and $\bar{m}\epsilon = m_\pi^2 f_\pi$.

m_0 (MeV)	500	600	700	800	900
g_1	15.4	14.8	14.2	13.3	12.3
g_2	8.96	8.43	7.76	6.94	5.92
$g_{\omega NN}$	11.4	9.12	7.31	5.67	3.54
$g_{\rho NN}$	8.05	6.97	7.46	7.75	8.75
$\bar{\mu}$ (MeV)	435	434	402	316	109
λ	40.5	39.4	34.5	22.5	4.26
λ_6	16.3	15.4	13.5	8.66	0.607

TABLE II. Physical inputs in vacuum (MeV).

m_+	m_-	m_ω	m_ρ	f_π	m_π
939	1535	783	776	93	140

III. DETERMINATION OF MODEL PARAMETERS

In this section, we determine the ten unknown parameters in this model by performing a global fit with chosen m_0 to masses and the pion decay constant in free space and to normal nuclear matter properties. In this global fitting we have used $m_0 = 900$, 800, 700, 600, and 500 MeV because we have found that with $m_0 = 400$ MeV or less we cannot reproduce the normal nuclear matter properties such as incompressibility.

The determined parameters are summarized in Table I. Now, we describe how we fix the model parameters and what the inputs are.

First, we determine six parameters by using the physical inputs listed in Table II. We choose the mass of positive-parity (negative-parity) nucleons as $m_+ = 939$ MeV ($m_- = 1535$ MeV). As in some literatures, one may also try $m_- = 1200$ MeV, but we have chosen the lightest and observed one. The pion mass and decay constant are $m_\pi = 140$ MeV and $f_\pi = 93$ MeV.

Next, the remaining parameters are fixed by the saturation density, the binding energy, the incompressibility, and the symmetry energy for the normal nuclear matter at zero temperature. The normal nuclear matter properties for the fit are discussed below, and empirical values of them are summarized in Table III.

[2]As we l explain in the next section, we use $m_+ = 939$ MeV and $m_- = 1535$ MeV as inputs to determine the values of g_1 and g_2 for given m_0. When we take m_+ as the mass of the negative-parity baryon and m_- as that of the positive-parity baryon, i.e., $m_- = 939$ MeV and $m_+ = 1535$ MeV, the determined values of g_1 and g_2 are exchanged. One can verify that this exchange does not cause any physical difference by swapping ψ_1 with ψ_2.

TABLE III. Physical inputs. $\mu_B^* = 923$ MeV. We took the values of incompressibility and symmetry energy from Refs. [38] and [33], respectively.

$\rho_0(\mu_B^*)$ (fm^{-3})	$E/A(\mu_B^*) - m_+$ (MeV)	K (MeV)	$E_{\rm sym}$ (MeV)
0.16	−16	240	31

The typical values of the nuclear saturation density and the binding energy are 0.16 fm^{-3} and −16 MeV, respectively. With $m_+ = 939$ MeV we have

$$\rho(\mu_B^* = 923\ \text{MeV}) = \rho_0 = 0.16\ \text{fm}^{-3}, \tag{3.1}$$

$$\left[\frac{E}{A} - m_+\right]_{\rho_0} = \left[\frac{\epsilon}{\rho_B} - m_+\right]_{\rho_0} = -16\ \text{MeV}. \tag{3.2}$$

We can consider another property of nuclear matter, the incompressibility, which is given by the curvature of binding energy at saturation density and corresponds to the "hardness" of the matter:

$$K = 9\rho_0^2 \frac{\partial^2 (E/A)}{\partial \rho^2}\bigg|_{\rho_0} = 9\rho_0 \frac{\partial \mu_B}{\partial \rho}\bigg|_{\rho_0}. \tag{3.3}$$

The symmetry energy per nucleon is from the difference of proton and neutron and is given as

$$E_{\rm sym}(\rho_B) = \frac{1}{2!}\frac{\partial^2 (E/A)}{\partial \delta^2} = \frac{1}{2!}\frac{\partial^2 (\epsilon/\rho)}{\partial \delta^2}, \tag{3.4}$$

where the asymmetry parameter δ is defined as

$$\delta \equiv \frac{\rho_p - \rho_n}{\rho_B} = \frac{2\rho_I}{\rho_B}. \tag{3.5}$$

We fit the remaining four parameters to the empirical values shown in Table III.

We would like to stress that we can reproduce the value of the incompressibility by the inclusion of the six-point interaction of the scalar meson σ, in contrast to the previous analyses by parity doublet models [19,23] where it seems difficult to reproduce the small value of the incompressibility.

IV. EQUATION OF STATE

In this section, we study the EOS for cold nuclear matter using the model constructed in the previous sections.

In Fig. 1, we show the dependence of the binding energy (a) and the pressure (b) on the baryon number density for $m_0 = 500$ MeV as an example.

The red line in Fig. 1(a) shows the dependence of the binding energy on the baryon number density of symmetric matter. From this, one can easily see that the binding energy is actually minimized at $\rho_B = \rho_0$, which implies that the existence of the bound nuclei and the saturation property are actually reproduced.[3]

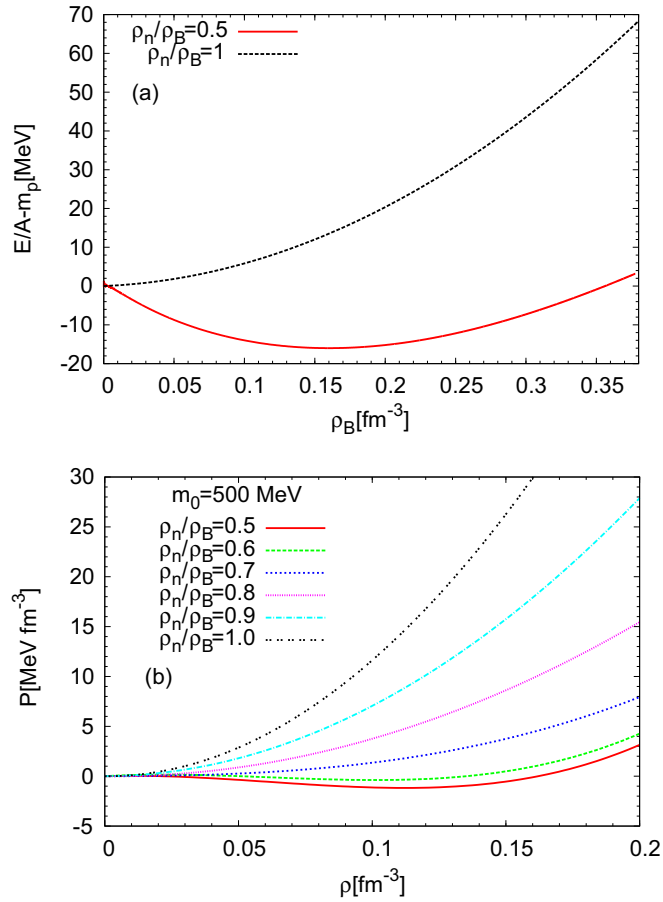

FIG. 1. (Color online) (a) Density dependence of the binding energy. (b) The pressure for $m_0 = 500$ MeV. ρ_B is the baryon number density and ρ_n is the neutron number density: $\rho_n/\rho_B = 0.5$ implies symmetric nuclear matter and $\rho_n/\rho_B = 1$ pure neutron matter.

Figure 1(b) shows that the pressure for $\rho_n/\rho_B = 0.5$ is negative in the low-density region, which means that the liquid phase of hadron coexists with the gas phase. In asymmetric matter, on the other hand, when the degree of asymmetry, ρ_n/ρ_B, is around $0.6 \sim 0.7$, the coexistence phase disappears and the pressure increases monotonically for larger asymmetry, which implies that the bound nuclei do not exist for $\rho_n/\rho_B > 0.7$.[4] In the case of the pure neutron matter ($\rho_n/\rho_B = 1$), the energy density as well as the pressure monotonically increases with the baryon number density. The EOS (pressure) of asymmetric nuclear matter is also discussed in molecular dynamics [39] and many-body perturbation [40]. Though our analysis is done within the mean-field approximation, the

[3]We would like to stress that we do not use the minimization condition as an input.

[4]Actually, the critical value of ρ_n/ρ_B depends on the chiral invariant mass: $\rho_n/\rho_B \sim 0.7$ for $m_0 = 500$ MeV and $\rho_n/\rho_B \sim 0.8$ for $m_0 = 900$ MeV.

TABLE IV. Predicted values of the slope parameter for $m_0 = 500$ to 900 MeV.

m_0 (MeV)	L (MeV)
900	75
800	74
700	78
600	78
500	75

qualitative behaviors in symmetric and neutron matter from Refs. [39,40] are similar to our result.

Next, we study the slope parameter, L, which is the gradient of the symmetry energy at the saturation density:

$$L = 3\rho_0 \frac{dE_{\rm sym}(\rho_B)}{d\rho_B}\bigg|_{\rho_B=\rho_0}. \tag{4.1}$$

The constraint for the value of L is obtained from some experiments, for example, heavy-ion collision experiments, nuclear masses, and so on [33,34]. In Table IV, we list our calculated values of the slope parameters for several choices of the chiral invariant mass m_0. This shows that the slope parameter hardly depends on m_0, all of which are within the allowed region shown in Refs. [33,34].

In Fig. 2, we show the dependence of the VEV of the σ field [panel (a)] and the baryon number density ρ_B [panel (b)] on the baryon number chemical potential μ_B for $m_0 = 500$ MeV in symmetric matter (red curves) and in the pure neutron matter (green curves).

Figure 2(a) shows that there are two points, $\mu_B \sim 900$ MeV and $\mu_B \sim 1300$ MeV, where the value of σ_0 changes rapidly. In the case of symmetric matter shown by the red curve, the first jump for $\mu_B \sim 900$ MeV can be identified with the first-order phase transition from the liquid phase to the gas phase as the baryon number density (an order parameter of the liquid-gas transition) undergoes sudden change around $\mu_B \sim 900$ MeV [see Fig. 2(b)].[5] Then, the phase transition around $\mu_B \sim 1300$ MeV can be naturally identified as the chiral phase transition. In symmetric nuclear matter (red dashed line), the liquid-gas phase transition is first order and there exists a coexistence phase. The existence of a coexistence phase in the nuclear liquid-gas phase transition has been confirmed in the experiments [41]. The coexistence phase in symmetric matter disappears by increasing μ_I, and the liquid-gas transition becomes second order as suggested in Ref. [6].

[5]One may schematically understand why the chiral condensate drops at the liquid-phase transition, where the baryon number density jumps as we increase the baryon chemical potential, through the Pauli exclusion principle. As the baryon density increases, the low-lying phase space relevant for quark-antiquark condensates is occupied by the fermions (quarks in nucleons in this case) that constitute the Fermi sea; therefore, forming quark-antiquark condensates requires much energy. At the liquid-gas transition point, there is a sudden increase in the number density, and so we could expect that the chiral (quark-antiquark) condensate changes drastically.

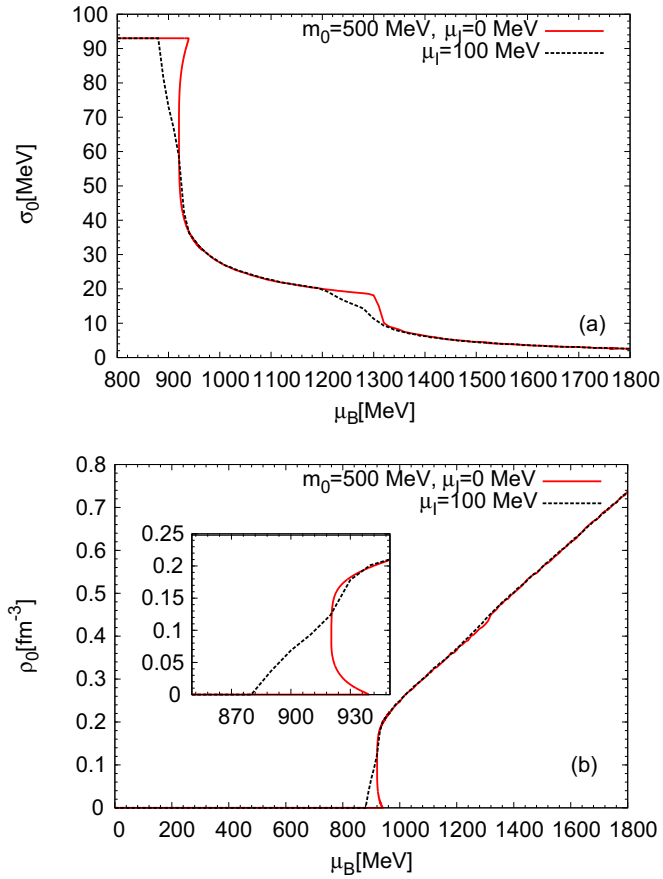

FIG. 2. (Color online) (a) Baryon number chemical potential dependence of σ_0. (b) Chemical potential dependence of ρ_B for $m_0 = 500$ MeV and $\mu_I = 0$ MeV.

Figure 3 shows the density dependence of the effective mass of the positive-parity (negative-parity) nucleon, m_+ (m_-). As ρ_B increases, m_+ and m_- gradually get close to the chiral invariant mass. This is a feature from parity doublet structure, and two nucleon masses degenerate to m_0 when

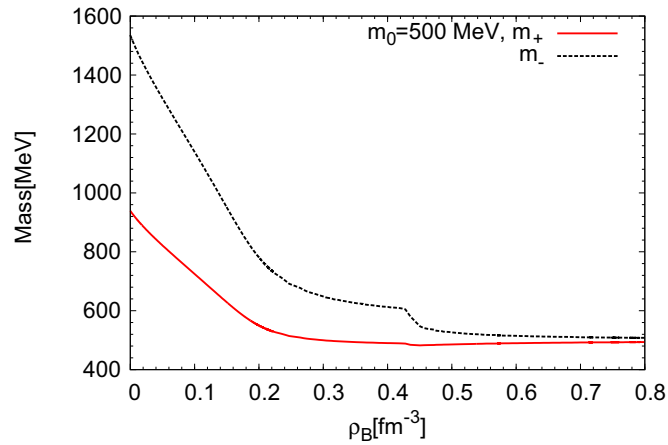

FIG. 3. (Color online) Density dependence of the effective nucleon masses for $m_0 = 500$ MeV at $\mu_I = 0$ MeV.

the chiral symmetry is completely restored. However, the mass difference between the parity partners remains finite in our model due to the current quark mass. The critical density for chiral symmetry restoration depends also on the chiral invariant mass, which is discussed in detail in the next section.

V. PHASE DIAGRAM

In this section, we explore the phase structure of our model at finite temperature and density with the isospin asymmetry. Our primary interest here is to see how the onset of the chiral and liquid-gas phase transition depends on the isospin asymmetry and the chiral invariant nucleon mass m_0. In this study, we do not consider the charged pion condensation, and so we take $|\mu_I| < m_\pi$.

Figure 4(a) corresponds to the phase diagram at $\mu_I = 0$, where we have the first-order liquid-gas phase transition (blue solid line) around $\mu_B = 900$ MeV and the chiral phase transition (red solid line) around $\mu_B = 1500$ MeV at zero and finite but small temperatures. The magenta dots are

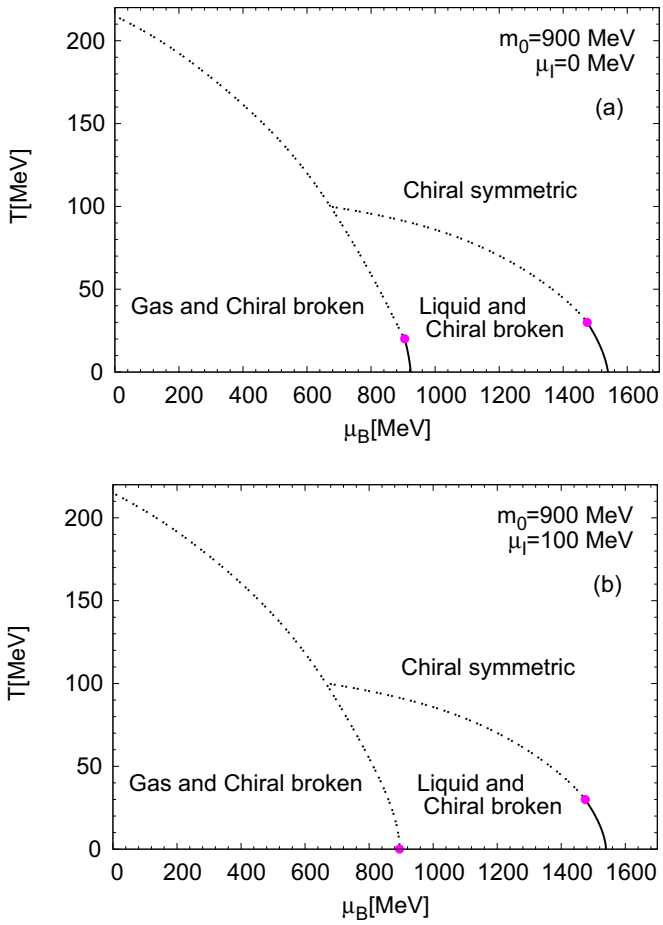

FIG. 4. (Color online) Phase diagrams for $m_0 = 900$ MeV at $\mu_I = 0$ MeV (a) and $\mu_I = 100$ MeV (b). The solid line is for the first-order phase transition, the dashed line for the crossover, and the point for the critical point (second order).

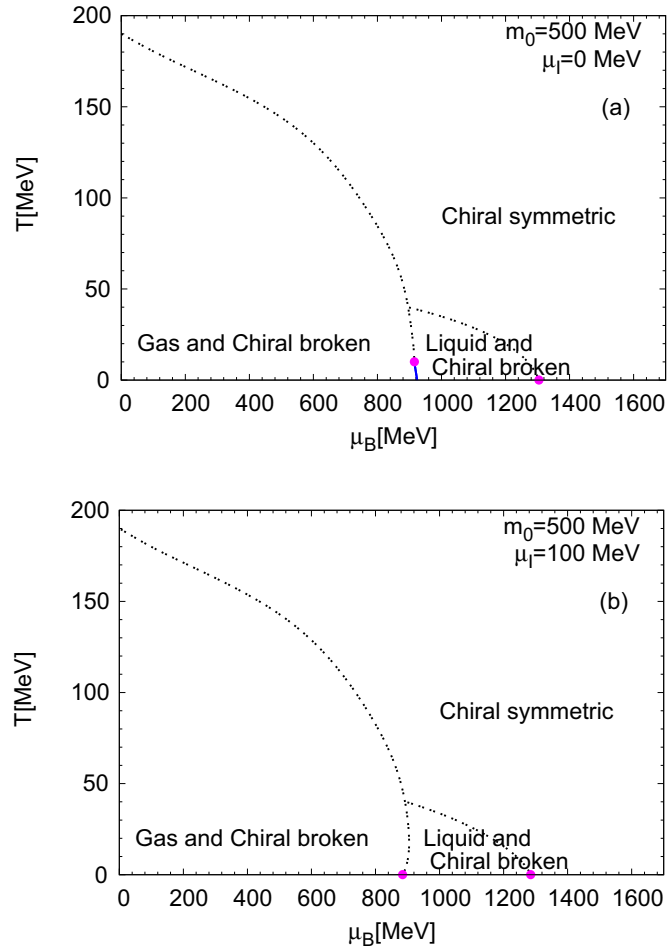

FIG. 5. (Color online) The phase diagrams for $m_0 = 500$ MeV.

second-order critical points, and the green dashed line shows the crossover.

The two crossover lines meet at a point around $(\mu_B, T) = (700\ \text{MeV}, 100\ \text{MeV})$ as seen in a study with a parity doublet model [23].

Figure 4(b) shows the phase diagram of asymmetric matter with $m_0 = 900$ MeV at $\mu_I = 100$ MeV. The trend of the liquid-gas and chiral phase transition is almost same as that of Figure 4(a) ($\mu_I = 0$); however, the liquid-gas transition becomes second order even at zero temperature as briefly mentioned in the previous section.

Now, we study how the chiral invariant mass affects the phase diagram. We take $m_0 = 500$ MeV as an example.

TABLE V. Critical values of the baryon chemical potential $\mu_B{}^c$ at $T = 0$ and $\mu_I = 0$ MeV.

m_0 (MeV)	$\mu_{B_{\text{lg}}}^c$ (MeV)	$\rho_{B_{\text{lg}}}^c$ (fm^{-3})	$\mu_{B_\chi}^c$ (MeV)	$\rho_{B_\chi}^c$ (fm^{-3})
900	923	0.16	1540	2.98
800	923	0.16	1643	1.75
700	923	0.16	1554	1.09
600	923	0.16	1426	0.69
500	923	0.16	1305	0.44

TABLE VI. Critical values of the baryon chemical potential and density at $T = 0$ and $\mu_I = 100$ MeV.

m_0 (MeV)	$\mu_{B^c_{\rm lg}}$ (MeV)	$\rho_{B^c_{\rm lg}}$ (fm^{-3})	$\mu_{B^c_\chi}$ (MeV)	$\rho_{B^c_\chi}$ (fm^{-3})
900	891	0.0	1537	2.98
800	891	0.0	1637	1.74
700	891	0.0	1543	1.09
600	888	0.0	1410	0.68
500	881	0.0	1285	0.43

Because the chiral invariant mass measures the amount of spontaneous chiral symmetry breaking needed for the nucleon masses and their mass splitting, we may expect that it mainly affects chiral symmetry in the phase diagram. The results are shown in Fig. 5. As expected, the nature of the liquid-gas transitions does not change, while the first-order chiral phase transition becomes second order.

Furthermore, as m_0 decreases, the critical density (chemical potential) for chiral transition decreases monotonically as summarized in Table V. Note that the saturation density is an input, and so is the corresponding chemical potential, in our study. This is why the critical density (chemical potential) for the liquid-gas phase transition does not change.

When we employ $m_0 = 900$ MeV, the critical density for chiral transition is about $17\rho_0$. On the other hand, the critical density becomes $\sim 3\rho_0$ with $m_0 = 500$ MeV. Comparing with a previous study in a parity doublet model with $m_0 = 800$ MeV [23], we find that our result for the symmetric matter is almost the same as the one from the previous study. Note, however, that we can explore the phase diagrams with the chiral invariant mass of the range 500 MeV $< m_0 <$ 900 MeV because we introduced the six-point interaction.

Table VI shows the critical baryon chemical potential and density for $\mu_I = 100$ MeV; comparing with Table V, we observe that the critical values become (slightly) smaller. Here the liquid-gas phase transition is second order so that $\rho_{B^c_{\rm lg}}$ must be 0.

VI. SUMMARY AND DISCUSSION

We have constructed a model for asymmetric nuclear matter by extending the parity doublet model. We introduced vector mesons (ρ and ω) through hidden local symmetry and also included the six-point interaction of the σ meson. We fixed our model parameters with chosen m_0 by performing a global fit to physical inputs (masses and pion decay constant in free space and nuclear matter properties). With the six-point potential, we were able to reproduce normal nuclear matter properties with m_0 in the range from 500 to 900 MeV.

We first studied the EOS and the phase diagram of dense symmetric matter at finite temperature. We observed that the slope parameter at the saturation density satisfies the constraint from heavy-ion experiments and neutron star observations, for instance, see Refs. [33,34], and found that the chiral condensate changes drastically at the chiral and liquid-gas transition points.

Then we considered asymmetric dense matter by adding a nonzero isospin chemical potential. We showed that the first-order nature of the liquid-gas transition disappears in asymmetric matter and the critical densities for the chiral transition become smaller with increasing isospin chemical potentials, which are in agreement with the results from existing literatures. We also showed that smaller chiral invariant nucleon mass favors smaller critical density for chiral phase transition in both symmetric and asymmetric dense matter.

Now, we discuss the chiral invariant nucleon mass. In our work, we chose the chiral invariant mass $m_0 = 500$–900 MeV to reproduce the properties of normal nuclear matter. However, the choice of chiral invariant mass is different in various studies. In Refs. [19,23], nuclear matter was studied in a parity doublet model and a rather large value of the chiral invariant mass was used, $m_0 \sim 900$ MeV. On the other hand, in Ref. [17] the authors determined m_0 from the decay width of $N^* \to N\pi$ to be $m_0 = 270$ MeV, while in Ref. [22] they used the decay modes of $N^* \to N\pi$ and $a_1 \to \pi\gamma$ to obtain $m_0 \sim 500$ MeV. These two studies were done in free space, and m_0 values from these studies are different from the one from nuclear matter studies as we mentioned in the Introduction. Our model can reproduce the nuclear matter properties even if $m_0 = 500$ MeV, which may imply that there is some possibility to reproduce vacuum and nuclear matter properties in a single model.

Recently, the study of parity doublet structure using lattice QCD [42] shows that the positive-parity nucleon mass changes very little near the deconfinement transition, which may imply that m_0 does exist in nature and its value is close to the positive-parity nucleon mass. The existence of chiral invariant mass is also discussed in the context of a Skyrmion crystal [43].

In this study, we do not consider interesting phenomena in dense (asymmetric) matter such as transition from nuclear matter to hyperonic matter (e.g., Refs. [25,26]), charged pion condensation with large isospin chemical potential, constraints from the neutron star mass-radius relation, and so on. These will be relegated to future works. Because the values of the chiral invariant mass are diverse in the literature, it is quite important and interesting to narrow down the value of m_0 and to dig further down to the role of m_0 in hadron physics.

ACKNOWLEDGMENTS

Y.M. would like thank to H. Nishihara for useful discussion during this work. The work of Y.M. is supported in part by the Nagoya University Program for Leading Graduate Schools funded by the Ministry of Education of the Japanese Government under Program No. N01. The work of Y.K. was supported by the Rare Isotope Science Project of the Institute for Basic Science funded by the Ministry of Science, ICT and Future Planning and by the National Research Foundation of Korea (Grant No. 2013M7A1A1075766). M.H. was supported in part by the JSPS Grants-in-Aid for Scientific Research (S) No. 22224003 and (C) No. 24540266.

[1] See, e.g. A. Akmal, V. R. Pandharipande, and D. G. Ravenhall, Phys. Rev. C **58**, 1804 (1998).
[2] P. Demorest, T. Pennucci, S. Ransom, M. Roberts, and J. Hessels, Nature (London) **467**, 1081 (2010).
[3] J. Antoniadis, P. C. C. Freire, N. Wex, T. M. Tauris, R. S. Lynch, M. H. van Kerkwijk, M. Kramer, C. Bassa *et al.*, Science **340**, 6131 (2013).
[4] M. Alford, M. Braby, M. W. Paris, and S. Reddy, Astrophys. J. **629**, 969 (2005).
[5] I. Bombaci and U. Lombardo, Phys. Rev. C **44**, 1892 (1991).
[6] H. Muller and B. D. Serot, Phys. Rev. C **52**, 2072 (1995).
[7] B. A. Li, C. M. Ko, and Z. Ren, Phys. Rev. Lett. **78**, 1644 (1997).
[8] F. Hofmann, C. M. Keil, and H. Lenske, Phys. Rev. C **64**, 034314 (2001).
[9] B. Liu, V. Greco, V. Baran, M. Colonna, and M. Di Toro, Phys. Rev. C **65**, 045201 (2002).
[10] W. Zuo, I. Bombaci, and U. Lombardo, Phys. Rev. C **60**, 024605 (1999).
[11] E. N. E. van Dalen, C. Fuchs, and A. Faessler, Phys. Rev. Lett. **95**, 022302 (2005).
[12] L. W. Chen, C. M. Ko, and B. A. Li, Phys. Rev. C **76**, 054316 (2007).
[13] P. Gogelein, E. N. E. van Dalen, K. Gad, K. S. A. Hassaneen, and H. Muther, Phys. Rev. C **79**, 024308 (2009).
[14] M. Drews and W. Weise, Phys. Rev. C **91**, 035802 (2015).
[15] J. Weyrich, N. Strodthoff, and L. von Smekal, arXiv:1504.02697.
[16] C. E. DeTar and T. Kunihiro, Phys. Rev. D **39**, 2805 (1989).
[17] D. Jido, M. Oka, and A. Hosaka, Prog. Theor. Phys. **106**, 873 (2001).
[18] T. Hatsuda and M. Prakash, Phys. Lett. B **224**, 11 (1989).
[19] D. Zschiesche, L. Tolos, J. Schaffner-Bielich, and R. D. Pisarski, Phys. Rev. C **75**, 055202 (2007).
[20] V. Dexheimer, S. Schramm, and D. Zschiesche, Phys. Rev. C **77**, 025803 (2008).
[21] V. Dexheimer, G. Pagliara, L. Tolos, J. Schaffner-Bielich, and S. Schramm, Eur. Phys. J. A **38**, 105 (2008).
[22] S. Gallas, F. Giacosa, and D. H. Rischke, Phys. Rev. D **82**, 014004 (2010).
[23] C. Sasaki and I. Mishustin, Phys. Rev. C **82**, 035204 (2010).
[24] S. Gallas, F. Giacosa, and G. Pagliara, Nucl. Phys. A **872**, 13 (2011).
[25] J. Steinheimer, S. Schramm, and H. Stocker, Phys. Rev. C **84**, 045208 (2011).
[26] V. Dexheimer, J. Steinheimer, R. Negreiros, and S. Schramm, Phys. Rev. C **87**, 015804 (2013).
[27] S. Benic, I. Mishustin, and C. Sasaki, Phys. Rev. D **91**, 125034 (2015).
[28] G. Colo, Phys. Part. Nucl. **39**, 286 (2008).
[29] U. Garg, Acta Phys. Pol., B **42**, 659 (2011).
[30] C. Sasaki, H. K. Lee, W. G. Paeng, and M. Rho, Phys. Rev. D **84**, 034011 (2011).
[31] W. G. Paeng, H. K. Lee, M. Rho, and C. Sasaki, Phys. Rev. D **85**, 054022 (2012).
[32] W. G. Paeng, H. K. Lee, M. Rho, and C. Sasaki, Phys. Rev. D **88**, 105019 (2013).
[33] J. M. Lattimer and Y. Lim, Astrophys. J. **771**, 51 (2013).
[34] C. J. Horowitz, E. F. Brown, Y. Kim, W. G. Lynch, R. Michaels, A. Ono, J. Piekarewicz, M. B. Tsang *et al.*, J. Phys. G **41**, 093001 (2014).
[35] M. Bando, T. Kugo, S. Uehara, K. Yamawaki, and T. Yanagida, Phys. Rev. Lett. **54**, 1215 (1985).
[36] M. Bando, T. Kugo, and K. Yamawaki, Phys. Rep. **164**, 217 (1988).
[37] M. Harada and K. Yamawaki, Phys. Rep. **381**, 1 (2003).
[38] S. Shlomo, V. M. Kolomietz, and G. Colo, Eur. Phys. J. A **30**, 23 (2006).
[39] J. A. Lopez, E. Ramirez-Homs, R. Gonzalez, and R. Ravelo, Phys. Rev. C **89**, 024611 (2014).
[40] C. Wellenhofer, J. W. Holt, and N. Kaiser, Phys. Rev. C **92**, 015801 (2015).
[41] J. Pochodzalla, T. Mohlenkamp, T. Rubehn, A. Schuttauf, A. Worner, E. Zude, M. Begemann-Blaich, T. Blaich *et al.*, Phys. Rev. Lett. **75**, 1040 (1995).
[42] G. Aarts, C. Allton, S. Hands, B. Jäger, C. Praki, and J.-I. Skullerud, Phys. Rev. D **92**, 014503 (2015).
[43] H. Dong, T. T. S. Kuo, H. K. Lee, R. Machleidt, and M. Rho, Phys. Rev. C **87**, 054332 (2013).